NAIC-ID(RS)T-0439-96

NATIONAL AIR INTELLIGENCE CENTER

MEASUREMENT OF ENERGY DISTRIBUTION AND ANALYSIS OF HAZARD PROBABILITY OF LONG-DISTANCE LASER IRRADIATION

by

Chen Zongli, Wang Denglong, et al.

HUMAN TRANSLATION

NAIC-ID(RS)T-0439-96 2 October 1996

MICROFICHE NR:

MEASUREMENT OF ENERGY DISTRIBUTION AND ANALYSIS OF HAZARD PROBABILITY OF LONG-DISTANCE LASER IRRADIATION

By: Chen Zongli, Wang Denglong, et al.

English pages: 15

Source: Laser Technology; pp. 308-313

Country of origin: China
Translated by: Leo Kanner Associates
F33657-88-D-2188
Requester: NAIC/TATD/Bruce Armstrong
Approved for public release: distribution unlimited.

GRAPHICS DISCLAIMER

All figures, graphics, tables, equations, etc. merged into this translation were extracted from the best quality copy available.

MEASUREMENT OF ENERGY DISTRIBUTION AND ANALYSIS OF HAZARD PROBABILITY OF LONG-DISTANCE LASER IRRADIATION

Chen Zongli, Wang Denglong, Xu Guidao, Shi Langshun
Zhang Guisu, Qian Huanwen, Zhou Shuying

Institute of Radiation Medicine,
Academy of Military Medical Sciences

ABSTRACT

To appreciate laser safety, we introduce a beam spot method of measuring long-distance laser irradiation. Based on laboratory eye injury data, we calculated the laser beam divergence, energy distribution over the laser cross section, and laser beam hazard probability.

With the ever-wider applications of laser technology and with advances in designing related equipment, such as laser ranging, laser communications, lidar, laser target indicators, etc., laser safety has become one of the critical issues faced by researchers. In particular, since the human eye focuses on the laser beam, low irradiation exposure may cause serious eye injuries.

Through long-distance atmospheric propagation, a field laser beam can basically produce two effects. One is energy attenuation due to light waves being absorbed and scattered by various elemental gases and aerosols in the atmosphere. The other effect is that the nonuniform values of atmospheric temperature, humidity,

pressure, and density may lead to random variations in atmospheric turbulence and atmospheric refractivity, followed by random fluctuations in the light wave parametric amplitude and phase. This will give rise to beam scintillation, splitting, drifting, bending, spreading, and image spot scintillation, as well as various atmospheric turbulence effects, including changes in beam polarization state, decrease of space coherence, etc. As a result, the characteristics of field long-distance laser beams are extremely complex, among which we may mention the laser beam divergence angle, beam spot size, and energy distribution over the laser beam cross section as all being important parameters for describing the output properties of laser devices.

It is understood that investigating the characteristics of the field long-distance laser beams is a complicated and difficult task, with heavy demands on materials and personnel. This paper introduced a long-distance field laser beam spot measurement method and in terms of safety, the authors calculated and analyzed the laser beam divergence angle, energy distribution over the laser cross section, laser-induced eye injury probability and extent, along with a comparison between the calculations and a field rabbit eye injury experiment. This method, simple, striking and with fewer factors giving rise to errors, has proven to be very much valuable to field laser safety protection and military-oriented applications.

1. MATERIAL AND METHOD

To record a complete contour of a field long-distance laser beam spot and to describe the energy distribution over the laser beam cross section, it is necessary to select an appropriate wavelength response, appropriate sensitivity and appropriate film size, based on photographic principles and laser beams operating at different wavelengths. In addition, the selected film must be tightly sealed, using a sealing case to prevent it from being

exposed. This paper studies an Nd:YAG frequency-multiplied 0.53μm green light using a visible-light-sensitive film. Actually, the laser beam still contains 1.06μm laser components even after frequency multiplication. However, the film is insensitive to the 1.06μm infrared laser light.

The measurement was conducted at night. Through repeated 1:1 recording of field long-distance beam spots on 50cmx60cm and 100cmx120cm large-size films, striking and true contours of long-distance laser beam spots were derived. During the measurements, a sufficiently large target plate was placed at a selected distance, and the laser device was adjusted to point at the target mark with the beam spot contour positioned at the target plate center. Then a selected film was placed on the target plate in a suitable position that faced the laser radiation direction. When everything had been done, the laser device was switched on to emit single pulses on the film, exposing it.

The exposed film was developed under extremely stringent conditions to make certain that the film was within the linear extent of the characteristic curve.

To quantitatively analyze the properties of the laser beam, the following procedures must be carried out during the measurements: (1) Record in detail several meteorological conditions including atmospheric visibility, temperature, humidity and wind force, etc.; (2) Conduct energy calibration. In doing so, one method is to find the most intensive radiation energy point in the beam thermal spot through repeated measurements over the entire beam cross section with an energy meter after film exposure, i.e., to measure the laser irradiance of the most intensive thermal spot in the laser beam. Another method is to measure the split ratio of the sample beam by using a beam splitting method, after which one beam serves for monitoring, while the other is used for exposure using a lensless camera, along with recording the exposure

irradiance $H_{\lambda\ standard}$. The film used here has the same characteristics as the large-size film. The standard sample beam spot filmed with the camera and the beam spot contour measured in the field are developed at the same time; (3) Measure the total laser output energy as well as the ratio between 1.06μm and 0.53μm laser light contained in the laser beam after frequency multiplication.

2. ESTIMATION OF BEAM SPOT AND BEAM DIVERGENCE ANGLE DERIVED THROUGH ACTUAL LONG-DISTANCE MEASUREMENTS

The field long-distance laser beam energy distribution is closely associated with beam pattern and divergence angle. Owing to the nonuniform energy distribution of the laser beam itself, the effect of atmospheric propagation and atmospheric turbulence, and particularly, the remarkable thermal spot effect caused by atmospheric scintillation, the long-distance beam spot becomes fuzzy. Figs. 1-4 show the contour of a typical beam spot measured at different distances between 0.8 and 2.5km under different meteorological conditions; Fig. 5 is a local thermal spot measured from a distance of 5.4km.

There are several ways of measuring and calculating the divergence angle. Based on the dimension of the beam spot measured from different distances, this paper estimated the laser beam divergence angle using Eq. (1) from the portion where energy is relatively concentrated; the direction of laser beam and its energy distribution extent at different distances was determined in approximate terms:

(1)

where R_1 and R_2 are the distances of laser beam propagation; a_1 and a_2, respectively, are the beam spot diameters at corresponding distances.

Fig. 1. Beam spot from a My-I laser device measured from a distance of 0.8km

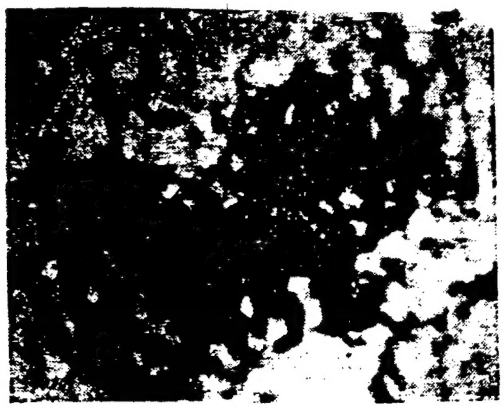

Fig. 2. Beam spot from a My-I laser device measured from a distance of 2.5km

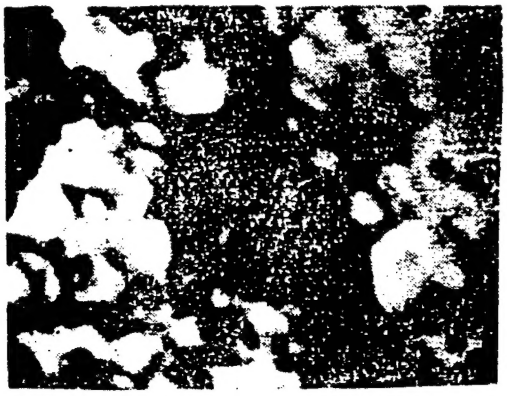

Fig. 3. Beam spot from an MG-I laser device measured from a distance of 1km

Fig. 4. Beam spot from an MG-II laser device measured from a distance of 5km

Fig. 5. Portion of a beam spot from an MG-II laser device measured from a distance of 5.4km

For safety reasons, the laser beam diameter a should be the diameter corresponding to the maximum irradiance 1/e. Actually, the true dimension of a beam spot can scarcely be determined and must only be estimated because a long-distance beam spot is highly irregular. Even so, it is still very significant in engineering applications for safety evaluation. From the measured beam spot, the beam divergence angle from a laboratory-oriented laser device was determined as to be less than 0.5mrad.

3. LIGHT DENSITY TEST

The dimension of the long-distance beam spot recorded in the field is extremely large: from 800 to 2500m including 180-600m at its center. To calculate the energy distribution throughout the beam cross section, first a light density test was conducted using a QTM-970 image analyzer developed by the British Cambridge Instrument Corporation[1]. For convenience in the hazard analysis,

the normal human pupillary diameter of 7mm under pupillary scattering or dark adaptation was selected as the beam spot diameter from the scanning beam of the instrument to scan the large-size film being photographed and to provide light density values at all levels, directly proportional to laser irradiance. Fig. 6 is a block diagram showing the operation of the image analyzer. Fig. 7 shows a histogram resulting from a light density test at all levels, which illustrates the test result over 1/4 of a beam spot measured at the distance of 2.15km.

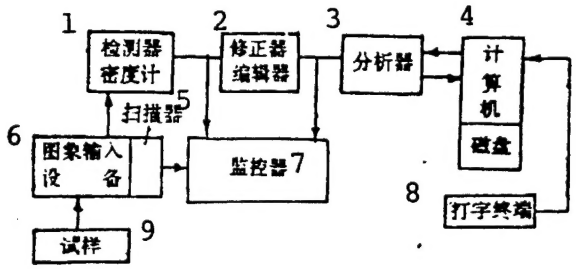

Fig. 6. Block diagram of QTM image analyzer
KEY: 1 - detector, densimeter 2 - corrector editor 3 - analyzer 4 - computer, disk 5 - scanner 6 - image input equipment 7 - monitor 8 - word processing terminal 9 - test sample

4. CALCULATIONS ON LASER BEAM ENERGY DISTRIBUTION PROBABILITY

Since atmospheric scintillation causes remarkable thermal spot effects, the energy distribution of a long-distance beam spot in space is extremely nonuniform. In terms of safety, turbulence action appears to be an uncertain variable in determining laser safety distance. On the one hand, turbulence may lead to diffraction of local beams in individual turbulent regions, resulting in beam expansion and increase of beam spreading angle. It is reported that if propagation distance increases by R, the beam spreading value of measurement will be $R^{3/2}$. Thus, when one's

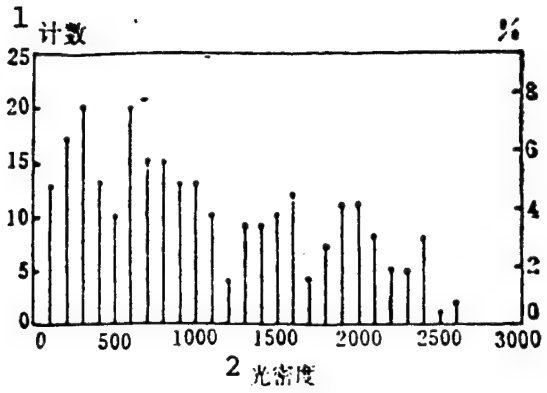

Fig. 7. Histogram for image analysis
KEY: 1 - counting 2 - light density

eyes are irradiated by laser beams, the retinal image may be enlarged and its energy density may decrease so that the eyes may be less damaged. From Fig. 5, the thermal spot 5.4km away has greatly been enlarged compared with the short-distance thermal spot. On the contrary, in some cases, when a laser beam passes through a turbulent region, its divergence angle may decrease even to not more than 0.3mrad to form a point light source, which can remarkably increase the eye injury distances.

For a Gaussian circular beam with an initial diameter a and beam spreading angle θ, the laser irradiance $H(J/cm^2)$ or irradiation $E(W/cm^2)$ at the distance R from the output end of the laser device can be calculated theoretically using Eqs. (2) and (3)

$$H=1.27Qe^{-\mu R}/(a+R\theta)^2 \qquad (2)$$

$$E=1.27\Phi e^{-\mu R}/(a+R\theta)^2 \qquad (3)$$

where Q, Φ, μ, respectively, are total laser output energy (J), total power (W), and atmospheric attenuation coefficient. A very large number of field tests confirmed that the irradiance (or irradiation) of the most intensive point in a long-distance thermal spot is far greater than its theoretical value. Table 1 lists the

theoretical calculations and actual measurements on a Nd:YAG laser rangefinder with an approximately 100mJ output and a 2mrad divergence angle[2].

TABLE 1. Comparison Between Actual Long-distance Measurement and Theoretical Calculations on a Rangefinder

1 距离 (m)	2 实测辐照量 (J/cm^2)	3 理论计算辐照量 (J/cm^2)
50	1.27×10^{-2}	9.97×10^{-4}
100	4.11×10^{-3}	2.89×10^{-4}
150	2.46×10^{-3}	1.36×10^{-4}
220	5.59×10^{-4}	6.25×10^{-5}
300	2.20×10^{-4}	3.41×10^{-5}
400	6.31×10^{-5}	1.91×10^{-5}

KEY: 1 - distance 2 - actually measured irradiance
3 - theoretically calculated irradiance

To study eye injuries from field laser beams at different distances, this paper adopted a most economical film recording method. Based on the laser irradiance calibrated at the same distances and under the same meteorological conditions during beam spot recording as well as the light density values measured with an image meter, the thermal spot energy distribution probability at different irradiation levels over corresponding distances can be calculated. The key problem in calculating energy distribution is to make certain that the recorded beam spots are not saturated during film development so that all the measured light density values lie within the linear range of the film characteristic curve, i.e., the light density values are directly proportional to laser irradiance. From the above description, there are two methods of calculating energy distribution in response to different

calibration methods. One method of calculating energy distribution is to measure the standard sample light density D_λ standard. Since the laser irradiance H_λ standard corresponding to the D_λ standard is known, the energy distribution can be directly calculated using Eq. (4) from the light density values measured by an image meter at different points. This method is referred to as an absolute method. The other method, called the relative method, can also calculate energy distribution using Eq (5) based on the maximum irradiance $H_{\lambda max}$ of the beam spot thermal point measured at the corresponding distance in the field, the maximum light density value $D_{\lambda max}$ in the measured beam spot and the light density value at a random point D_i as follows:

$$\frac{D_{\lambda 标}^{*}}{H_{\lambda 标}^{*}} = \frac{D_i}{H_i} \qquad H_i = \frac{H_{\lambda 标}^{*}}{D_{\lambda 标}^{*}} D_i = A_1 D_i \tag{4}$$

$$\frac{D_{\lambda max}}{H_{\lambda max}} = \frac{D_i}{H_i} \quad , \quad H_i = \frac{H_{\lambda max}}{D_{\lambda max}} \cdot D_i = A_2 D_i \tag{5}$$

KEY: * = standard

Tables 2 and 3 show the calculations of energy distribution of beam spots with a 0.3mrad divergence angle, emitted from MG-I and MG-II laser devices (Figs. 3 and 4) over distances of 1km and 2.15km.

5. ANALYSIS OF FIELD LONG-DISTANCE LASER BEAM HAZARD PROBABILITY

Hazard probability means finding the energy distribution percentage above the ocular injury threshold (or injury irradiance) level in the entire beam spot and evaluating laser beam hazard probability and extent of hazard to human eyes, based on the study of field long-distance beam spot energy distribution and laser thresholds. Similarly, the long-distance laser safety probability and safety extent can also be studied in accordance with the laser safety standard.

TABLE 2. MG-I Laser Beam Spot Energy Distribution at 1km

0.53μm激光辐照量 (μJ/cm²) 1	辐照量分布比例 (%) 2	3 注
3.3～13.6	19.8	4能见度
13.6～23.2	13.1	7km
23.2～33.1	11.8	
33.1～43.1	9.8	
43.1～53.1	10.2	
53.1～66.3	12.3	
66.3～76.3	7.5	
76.3～86.3	8.3	
86.3～92.6	3.5	
92.6～99.4	3.6	

KEY: 1 - laser irradiance 2 - irradiance distribution percentage 3 - remarks 4 - visibility

Table 4 shows the study results of the experiment-oriented 0.53μm multiple frequency light thresholds[3]. Through weighing and regression of these results, the eye injury dose E_{D1} and E_{D50} values can be obtained. Table 5 shows a derivation of long-distance beam spot hazard probability based on thresholds and energy distribution at different distances along with a comparison between the calculations and a field rabbit eye biological effect experiment.

According to Table 5, the irradiance of beam spots emitted from an MG-I laser device 1km away is greater than that of rabbit eyes E_{D1} and E_{D50}, respectively, by percentages of 81% and 52.7%, while in the rabbit eye injury experiment conducted at the same distance, the injury generation rate is 54.5%. At the distance of 2.15km, the beam spot energy distribution is greater than E_{D1} and

TABLE 3. MG-II Laser Beam Spot Energy Distribution at 2.15km

0.53μm激光辐照量[1] (μJ/cm²)	辐照量分布比例[2] (%)	注[3]
1.82～ 7.27	8.9	[4] 能见度
7.27～12.71	8.4	20km
12.71～18.16	11.1	
18.16～23.61	9.4	
23.61～29.06	8.8	
29.06～34.51	8.7	
34.51～39.96	10.5	
39.96～45.40	10.6	
45.40～50.85	20.2	
50.85～54.48	3.3	

KEY: 1 - laser irradiance 2 - irradiance distribution percentage 3 - remarks 4 - visibility

E_{D50} by 82.6% and 40.2%, respectively, while in the rabbit eye injury experiment, the injury rate is 25.4%. It is to be noted that the animal experiment was not made in the entire beam spot range and therefore, the injury generation rate suggested was only a result of irradiation from local thermal spots. Obviously, the experiment and calculations were carried out under different conditions but did not show any contradiction.

6. CONCLUSIONS

1. Atmospheric turbulence has a great effect on the ground surface. The degree of atmospheric turbulence is determined by the structural constant of atmospheric refractivity C_N, while C_N changes at any time within a range from $5\times10^{-8}m^{-1/3}$ to $10^{-6}m^{-1/3}$, basically related to the temperature gradient on the ground

TABLE 4. 0.53μm Laser Eye Injury Threshold

种属 1	分组 2	3平均角膜辐照量(J/cm²)	4眼损伤(%)	注 5
6 兔	1	1.44×10^{-5}	0	$E_{1}=0.99$
	2	1.824×10^{-5}	15.9	$\times 10^{-5}$
	3	2.265×10^{-5}	14.6	(J/cm²)
	4	2.826×10^{-5}	34.5	$E_{D50}=$
	5	3.592×10^{-5}	40.7	$3.92\times$
	6	4.408×10^{-5}	58.8	10^{-5}
	7	5.551×10^{-5}	69.2	(J/cm²)
	8	7.005×10^{-5}	86.2	

KEY: 1 - species 2 - group 3 - average corneal irradiance 4 - eye injury 5 - remarks 6 - rabbit

surface. Turbulence reaches its highest value on sunny days when there is intensive solar radiation and surface heat rises. While on cold cloudy days or at night, turbulence is weak. In windy days when wind mixes with air, the turbulent regions can be seen swiftly passing through, under blowing wind, the beam spot, compelling the scintillation spot to rise and fall with the wind and causing the energy distribution to vary irregularly. The general size of a scintillation spot is often illustrated with a horizontal correlation distance ( )[4], i.e., with increase in beam propagation distance R, the thermal spot increases with the square root of the product of R and wavelength λ. Fig. 5 shows a part of a beam spot measured at the distance of 5.4km, whose thermal spot effect appears more striking than the short-distance spots. In addition, the effect of turbulence becomes smaller at short distances and at a height over 10km above the ground surface. Obviously, when a laser beam is emitted in air or from ground to air, its turbulence effect is much smaller than on the ground.

TABLE 5. Field Laser Beam Spot Hazard Probability

1 型号	2 距离 (km)	3 能见度 (km)	0.53μm 4 光最大辐照量 (μJ/cm²)	≥$E_{5.1}$ 5 辐照量 (%)	≥$E_{D5.0}$ 6 辐照量 (%)
MG-I	1.0	7.0	99.4	81	52.7
MG-II	2.15	20	54.4	82.6	40.2

KEY: 1 - model 2 - distance 3 - visibility
4 - 0.53μm laser maximum irradiation
5 - irradiance 6 - irradiance

2. The key to increasing the reliability of calculations is to strictly control film development conditions so that the measured light density values lie within the linear range of the film characteristic curve. Secondly, since there are many factors that may affect the stability of laser device output in the field, it is necessary to carefully and repeatedly conduct measurements during calibration so as to satisfy engineering applications.

3. This paper mainly discusses a method of recording beam spots with visible light films. However, the near-infrared and far-infrared wavebands are even more difficult to record. 1.06μm and 10.6μm laser beams were tentatively studied in the laboratory and corresponding methods were also invented, but they are yet to be applied in field conditions.

REFERENCES

1. Zhang Zhengsheng, "Image Analysis," Instrument Test Center, Academy of Military medical Sciences, 1985: 3.

2. Chen Zongli, Laser Technology, 1987; 11(2): 38.

3. Xu Jiemin, Zhou Shuying, Hu Fugeng (dec.) et al., China Laser, 1985; 12(10): 618.

4. Sliney, D. and M. Wolbarsht, Safety with Lasers and Other Optical Sources-A Comprehensive Handbook, Plenum Press, N.Y. and London, 1980: 415.

About the Author

Chen Zongli, male, born in April, 1934, is a senior engineer now engaged in research on laser measurement and protection.

This paper was received for editing on December 17, 1991. The edited paper was received on March 30, 1992.